Articles

Chemical Force Microscopy on Single-Walled Carbon Nanotube Paper

Mark A. Poggi,[†] Peter T. Lillehei,[‡] and Lawrence A. Bottomley*,[†]

School of Chemistry and Biochemistry, Georgia Institute of Technology, Atlanta, Georgia 30332-0400, and NASA Langley Research Center, Advanced Materials and Processing Branch, Hampton, Virginia 23681-2199

Received September 21, 2004. Revised Manuscript Received May 28, 2005

Topographical and adhesive force measurements were acquired simultaneously on single-walled carbon nanotube (SWNT) paper using chemically modified atomic force microscopy probe tips. Gold-coated cantilever probe tips were chemically modified with a series of ω-substituted alkanethiols or *para*-substituted arylthiols. The observed adhesion forces were highly dependent on the contact area between the tip and paper, the type of thiol (alkane versus aryl), and the identity of the terminal group. The adhesion force per molecule interacting with the sidewall of single-walled carbon nanotubes was elucidated after correcting for variations in tip shape and sample topology.

Introduction

Carbon nanotubes possess a unique combination of electrical, thermal, and mechanical properties[1−3] that has prompted a global investigation of their use in polymeric composites. If reliable methods for aligning and distributing the nanotubes in a polymer matrix can be found, an unprecedented lightweight, high-strength, and thermally and electrically conductive material will result. With present composite fabrication methods, nanotube aggregation is commonplace, leading to composites with less than optimal properties and unacceptable defect densities. Current techniques applicable for studying the dispersion of nanotubes within the composite are scanning electron microscopy and magnetic force microscopy.[4,5]

To increase dispersal of nanotubes in the polymer by reducing aggregation, researchers have chemically modified the nanotubes. While the dispersion of the tubes has been enhanced using this approach, the electrical conductivity has been significantly reduced.[6−10] Chemical modification results in a change in the hybridization of the carbon in the nanotube from sp^2 to sp^3, resulting in a significant reduction in the electron transport properties of the nanotube. Composites made with chemically modified nanotubes would thus be appropriate for applications where electrical conductivity is not desired (i.e., the nanotubes serve strictly as a reinforcing agent).

Research is ongoing to find ways to disperse nanotubes without covalent modification.[11−13] If polymers can be tailored to enhance the dispersal of the nanotubes and not sacrifice their conductive properties, viable composites for space applications will become a reality. To date, only a few theoretical and experimental studies have been reported on the chemical and physical interactions at the nanotube/polymer interface.[14−18] In our view, a better understanding of the interfacial chemistry between carbon nanotubes and polymeric materials will aid in the dispersal of nanotubes into polymer composites and yield materials that have uniformly distributed electrical and mechanical properties.

* Corresponding author. E-mail: lawrence.bottomley@chemistry.gatech.edu. Phone: (404)894-4014. Fax: (404)385-6447.
[†] Georgia Institute of Technology.
[‡] NASA Langley Research Center.

(1) Dai, H. *Acc. Chem. Res.* **2002**, *35*, 1035−1044.
(2) Qian, D.; Wagner, G. J.; Liu, W. K.; Yu, M.; Ruoff, R. S. *Appl. Mech. Rev.* **2002**, *55*, 495−533.
(3) Salvetat-Delmotte, J.; Rubio, A. *Carbon* **2002**, *40*, 1729−1734.
(4) Ajayan, P. M.; Schadler, L. S.; Giannaris, C.; Rubio, A. *Adv. Mater.* **2000**, *12*, 750−753.
(5) Lillehei, P. T.; Park, C.; Rouse, J. H.; Siochi, E. J. *Nano Lett.* **2002**, *2*, 827−829.
(6) Eitan, A.; Jiang, K.; Dukes, D.; Andrews, R.; Schadler, L. S. *Chem. Mater.* **2003**, *15*, 3198−3201.
(7) Boul, P. J.; Liu, J.; Mickelson, E. T.; Huffman, C. B.; Ericson, L. M.; Chiang, I. W.; Smith, K. A.; Colbert, D. T.; Hauge, R. H.; Margrave, J. L.; Smalley, R. E. *Chem. Phys. Lett.* **1999**, *310*, 367−372.
(8) Chen, J.; Hamon, M. A.; Hu, H.; Chen, Y.; Rao, A. M.; Eklund, P. C.; Haddon, R. C. *Science (Washington, DC)* **1998**, *282*, 95−98.
(9) Kamaras, K.; Itkis, M. E.; Hu, H.; Zhao, B.; Haddon, R. C. *Science (Washington, DC)* **2003**, *301*, 1501.
(10) Strano, M. S.; Dyke, C. A.; Usrey, M. L.; Barone, P. W.; Allen, M. J.; Shan, H.; Kittrell, C.; Hauge, R. H.; Tour, J. M.; Smalley, R. E. *Science (Washington, DC)* **2003**, *301*, 1519−1522.
(11) Rouse, J. H.; Lillehei, P. T.; Sanderson, J.; Siochi, E. J. *Chem. Mater.* **2004**, *16*, 3904−3910.
(12) Park, C.; Ounaies, Z.; Watson, K. A.; Crooks, R. E.; Smith, J.; Lowther, S. E.; Connell, J. W.; Siochi, E. J.; Harrison, J. S.; Clair, T. L. S. *Chem. Phys. Lett.* **2002**, *364*, 303−308.
(13) Ounaies, Z.; Park, C.; Wise, K. E.; Siochi, E. J.; Harrison, J. S. *Composites Sci. Technol.* **2003**, *63*, 1637−1646.
(14) Barber, A. H.; Cohen, S. R.; Wagner, H. D. *Phys. Rev. Lett.* **2004**, *92*, 186103/186101−186103/186104.
(15) Barber, A. H.; Cohen, S. R.; Wagner, H. D. *Appl. Phys. Lett.* **2003**, *82*, 4140−4142.
(16) Cooper, C. A.; Cohen, S. R.; Barber, A. H.; Wagner, H. D. *Appl. Phys. Lett.* **2002**, *81*, 3873−3875.
(17) Liao, K.; Li, S. *Appl. Phys. Lett.* **2001**, *79*, 4225−4227.
(18) Wagner, H. D. *Chem. Phys. Lett.* **2002**, *361*, 57−61.

10.1021/cm048346m CCC: $30.25
Published on Web 07/23/2005

Chemical force microscopy (CFM) is an extremely versatile technique for examining interfacial interactions between two chemically modified surfaces.[19] With chemical modification of an AFM cantilever tip and use of it to probe the sidewalls of SWNTs, the interfacial interactions between the sidewall of a nanotube and the chemical moieties that comprise the backbone and side chains of polymers commonly used in composites can be measured. We have previously reported on the suitability of CFM for investigating the interfacial chemistry of SWNT paper.[20,21] In this report, we build upon our preliminary results and present a thorough and systematic investigation of the interfacial interactions between SWNT paper and gold-coated cantilever probe tips chemically modified with a series of ω-substituted alkanethiols and *para*-substituted benzenethiols.

Experimental Section

Materials. All experiments were carried out on purified SWNT paper obtained from the Advanced Materials and Processing Branch, NASA Langley Research Center. This paper was prepared according to Liu's method.[22] The following alkanethiols were used as received from the supplier: 11-amino-undecanethiol (Dojindo Chemicals), 1*H*,1*H*,2*H*,2*H*-perfluorodecane-1-thiol (FluroFlash), 11-dodecanethiol, 11-mercaptoundecanoic acid, and 1,6-hexanedithiol (Sigma-Aldrich). The following alkanethiols were synthesized according to literature methods: bis(11-hydroxyundecyl)disulfide[23] and 11-undecenethiol.[24] The purity of these two materials was verified by mass spectrometry and both ^{1}H and ^{13}C nuclear magnetic resonance spectroscopy. The following *para*-substituted benzenethiols were used as received from the supplier: 4-mercaptobenzonitrile (Apin Chemicals Ltd.), 4-bromobenzenethiol, 4-methylbenzenethiol, 4-nitrobenzenethiol, benzenethiol, 4-methoxybenzenethiol, 4-fluorobenzenethiol, 4-mercaptophenol, and 4-amino-benzenethiol (Sigma-Aldrich). The cantilevers (NSC 12) were obtained from MikroMasch.

Instrumentation. AFM-based adhesion measurements were carried out with a Nanoscope IIIa Extended MultiMode IIIa scanning probe microscope (Veeco Metrology) operated in "Force Volume" mode. All piezoelectric scanners were calibrated in *x*, *y*, and *z* with NIST-certified calibration gratings (MikroMasch). Force constants for the cantilevers were acquired via the thermal resonance method[25,26] using the Signal Access Module (Veeco Metrology) and a Model SR785 Dynamic Signal Analyzer (Stanford Research Systems). Force constants ranged from 0.7 to 1.2 N/m. The tip radius of each cantilever was determined using tip-deconvolution software (SPIP by Image Metrology). All experiments were performed under a custom-built nitrogen atmosphere to reduce the relative humidity to less than 2%.[27,28]

Scanning electron micrographs were obtained on an Hitachi S-5200 high-resolution scanning electron microscope. Samples were mounted on aluminum stubs using graphite paste. Images were acquired at an accelerating voltage of 1.0 eV.

Methods. A thin film of gold was evaporated onto both sides of the cantilevers to enable chemical functionalization of the probe tip by self-assembly of alkane- or arylthiols. To prepare chemically modified probe tips, cantilevers were first cleaned in "piranha solution", thoroughly rinsed in ethanol, and then placed into a 1 mM solution of the desired thiol dissolved in filtered absolute ethanol or filtered hexane (Sigma-Aldrich) for a period of 3−24 h. All of the alkane- and benzenethiols used herein are known to form well-ordered monolayers.[29] Upon removal of the cantilever from the self-assembling thiol solution, the cantilever was thoroughly rinsed in the same solvent used to prepare the thiol solution, dried in vacuo, and then stored under nitrogen until use.[30]

Adhesion measurements were made in "force volume mode" using the relative triggering option. (Readers desiring a more detailed description of force volume imaging are referred to the Veeco Metrology application note entitled "Applications of Force Volume Imaging with Atomic Force Microscopes".) Force and topographic images were acquired using a 50 × 50 nm scan domain at 256 pixels per image. The same loading rate was used in all force spectroscopic measurements (200 nN/s, scanner *z*-velocity = 400 nm/s). Force volume images were acquired at a minimum of 10 randomly chosen locations on the SWNT paper for each chemically modified tip. Cantilever deflection versus scanner/sample position data was extracted from the NanoScope IIIa data file and imported into a Microsoft Excel spreadsheet using a data extraction program written in Visual Basic based on the one reported by Eaton et al.[31,32] Macros written in Excel converted individual force curves from deflection vs point number to force vs separation format and calculated the force at maximum tip deflection (i.e., adhesion force). Adhesion forces were mapped relative to the position of the tip over the SWNT paper.

Results and Discussion

The single-walled nanotube paper used herein was prepared by Prof. Richard E. Smalley's group at Rice University according to their previously reported method.[22] The paper consisted of single-walled nanotube ropes and bundles of ropes. Figure 1 depicts scanning electron microscope (SEM) images of the paper and verifies the presence of a high number of tubes and bundles per unit area. Prior to force volume imaging, the SWNT paper was imaged in Tapping Mode using an uncoated cantilever to locate areas on the paper that possessed a high density of tubes/bundles per unit area. A typical image is depicted in Figure 2. This image reveals the presence of individual nanotubes as well as nanotube ensembles (intertwined tubes, bundles, and ribbons). Once areas with a high number of individual nanotubes were located, the chemically modified cantilever was mounted into the AFM and force volume measurements were performed.

(19) Noy, A.; Vezenov, D. V.; Lieber, C. M. *Annu. Rev. Mater. Sci.* **1997**, *27*, 381−421.
(20) Bottomley, L. A.; Poggi, M. A.; Lillehei, P. T. *Proc.−Electrochem. Soc.* **2003**, *2003−15*, 297−304.
(21) Poggi, M. A.; Bottomley, L. A.; Lillehei, P. T. *Nano Lett.* **2004**, *4*, 61−64.
(22) Liu, J.; Rinzler, A. G.; Dai, H.; Hafner, J. H.; Bradley, R. K.; Boul, P. J.; Lu, A.; Iverson, T.; Shelimov, K.; Huffman, C. B.; Rodriguez-Macias, F.; Shon, Y.-S.; Lee, T. R.; Colbert, D. T.; Smalley, R. E. *Science (Washington, DC)* **1998**, *280*, 1253−1256.
(23) Bottomley, L. A.; Jones, J. A.; Ding, Y.; Allison, D. P.; Thundat, T.; Warmack, R. J. *SPIE Proc. Biomed. Opt. Soc.* **1993**, *1891*, 48−55.
(24) Bain, C. D.; Troughton, E. B.; Tao, Y. T.; Evall, J.; Whitesides, G. M.; Nuzzo, R. G. *J. Am. Chem. Soc.* **1989**, *111*, 321−335.
(25) Butt, H.-J.; Jaschke, M. *Nanotechnology* **1995**, *6*, 1−7.
(26) Hutter, J. L.; Bechhoefer, J. *Rev. Sci. Instru.* **1993**, *64*, 1868−1873.
(27) Patton, S. T.; Eapen, K. C.; Zabinski, J. S. *Tribol. Int.* **2001**, *34*, 481−491.
(28) Willing, G. A.; Neuman, R. D. *Langmuir* **2002**, *18*, 8370−8374.
(29) Porter, M. D.; Bright, T. B.; Allara, D. L.; Chidsey, C. E. D. *J. Am. Chem. Soc.* **1987**, *109*, 3559−3568.
(30) Nan, X.; Gu, Z.; Liu, Z. *J. Colloid Interface Sci.* **2002**, *245*, 311−318.
(31) Eaton, P.; Fernandez Estarlich, F.; Ewen, R. J.; Nevell, T. G.; Smith, J. R.; Tsibouklis, J. *Langmuir* **2002**, *18*, 10011−10015.
(32) Eaton, P.; Smith, J. R.; Graham, P.; Smart, J. D.; Nevell, T. G.; Tsibouklis, J. *Langmuir* **2002**, *18*, 3387−3389.

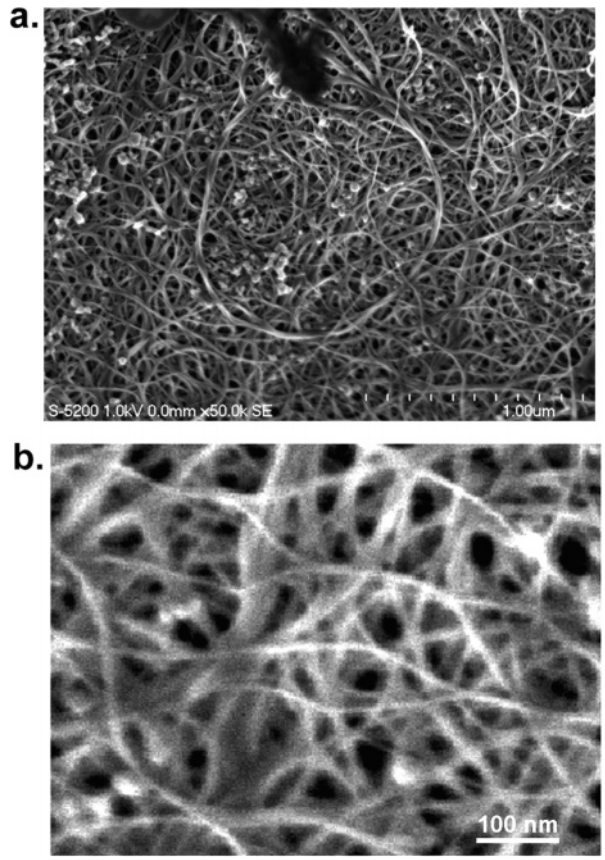

Figure 1. Scanning electron micrographs of SWNT paper prepared by the HiPco process at low (a) and high (b) magnification.

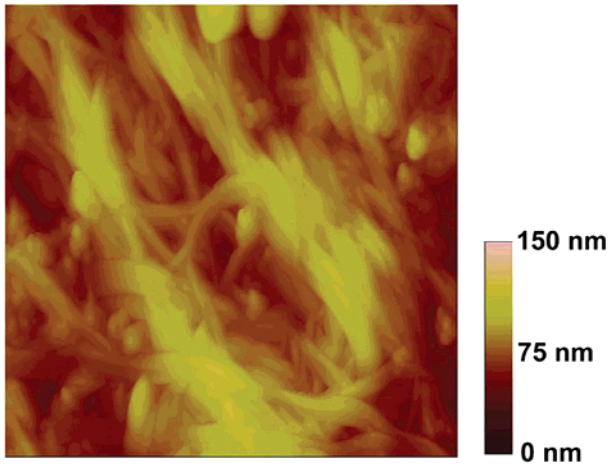

Figure 2. Tapping Mode AFM image of SWNT paper. Image domain is 1 μm × 1 μm.

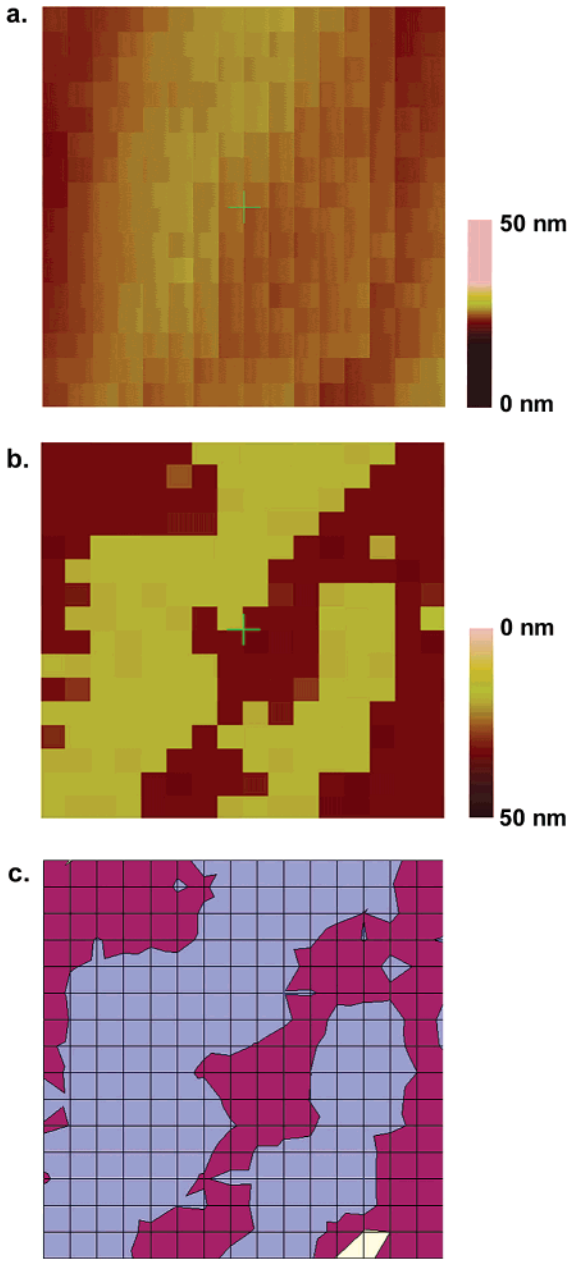

Figure 3. (a) Highly pixelated topographical image acquired in force volume mode using a cantilever tip modified with a hydroxyl-terminated alkanethiol (50 nm × 50 nm scan size). (b) Force−volume image acquired simultaneously with the topographical image. (c) Adhesion map generated from the individual force curves measured at each pixel in the image. The contrast in the adhesion map is blue represents an adhesive force from 0 to 4 nN, maroon 4−8 nN, and yellow 8−12 nN.

Adhesion Mapping of SWNT Paper. Figure 3a is a topographical image acquired in force volume mode at higher magnification with a cantilever derivatized with a hydroxyl-terminated thiol. Figure 3b is the force volume image acquired in parallel with the topographical image. Each pixel corresponds to an individual force measurement. Force−separation curves were extracted from force volume images and from these adhesion forces were calculated from the point of maximum cantilever deflection. Figure 3c depicts a mapping of the adhesion force relative to the position of the tip over the nanotube paper. The figure was generated by point-by-point multiplication of the spring constant of the cantilever multiplied by the cantilever's maximal deflection.

Figure 4a is a histogram plot of the adhesion force at rupture of the hydroxyl-terminated alkanethiol-modified cantilever during force volume imaging of the SWNT paper. A bimodal distribution of the forces, one band centered at 5 nN and the other at 12 nN, is present in the data. Histograms summarizing the adhesion forces obtained during force volume imaging with other alkanethiols are also presented in Figure 4. For these, mono-, bi-, or trimodal distributions of forces are obtained. The average rupture force (and standard deviation) was determined for each thiol; the data are presented in the first two columns of Table 1. Adhesive interactions ranged from 5.5 ± 3.4 to 11.7 ± 5.6 nN for the perfluoro- and amino-terminated alkanethiols, respectively.

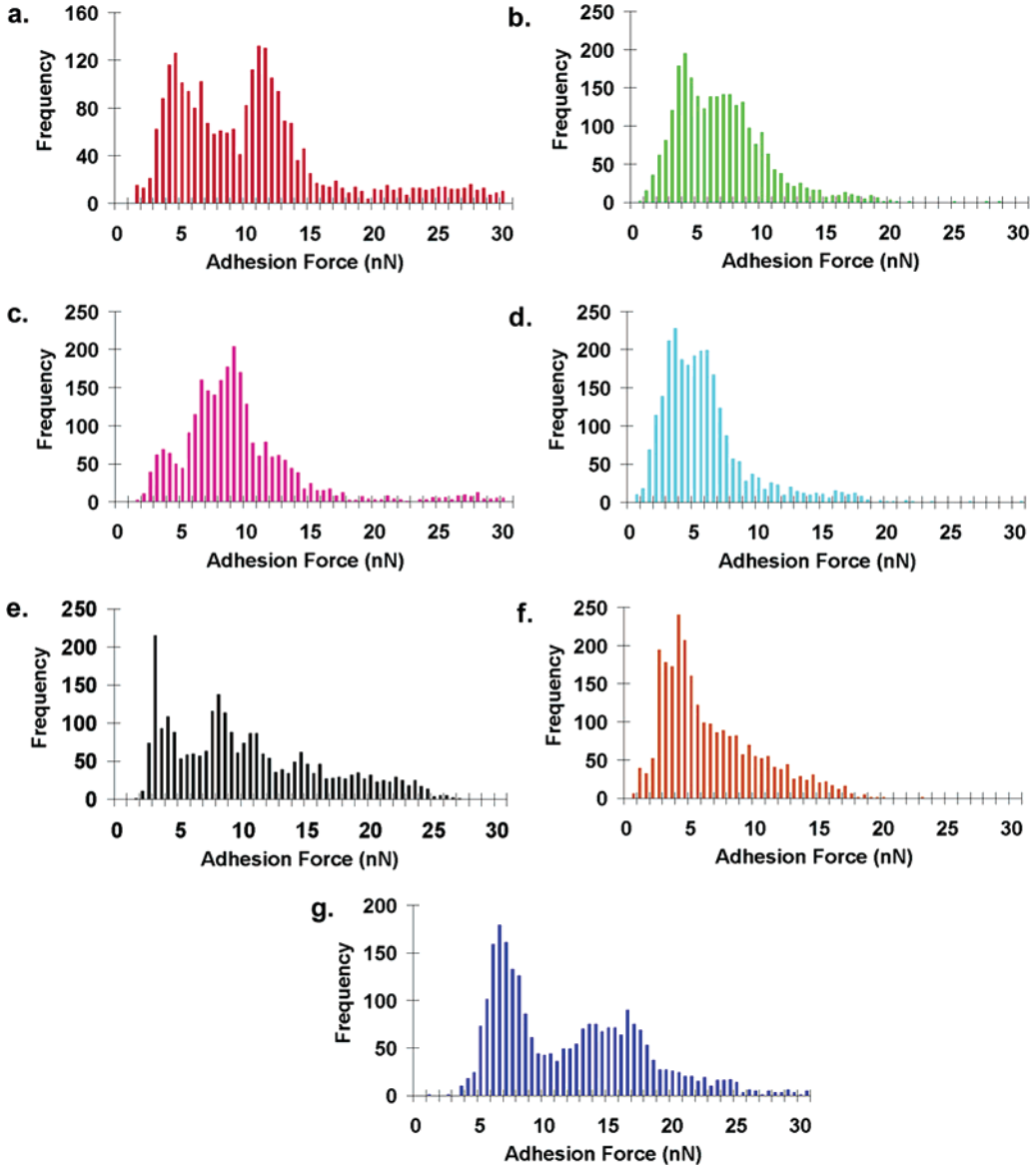

Figure 4. Histograms showing the distribution of forces required to detach a chemically modified cantilever tip from the SWNT paper. The tips were chemically modified with the following series of ω-substituted alkanethiols: (a) 11-hydroxy-undecanethiol, (b) 11-dodecanethiol, (c) 11-mercaptoundecanoic acid, (d) 1*H*,1*H*,2*H*,2*H*-perfluorodecane-1-thiol, (e) 11-undecenethiol, (f) 1,6-hexanedithiol, and (g) 11-amino-undecanethiol.

Table 1. Summary of Adhesion Forces between SWNT Paper and the Cantilever Tip Modified with ω-Substituted Alkanethiols

thiol end group	average rupture force[a] (nN)	force/radius[b] (pN/nm)	no. of force curves[c]	adhesion force[d] (pN/molecule)
$-CH_3$	6.9 ± 6.5	150 ± 40	142	7.6 ± 2.0
−SH	6.2 ± 3.8	110 ± 40	1185	8.2 ± 2.6
−perfluoro	5.5 ± 3.4	120 ± 40	863	8.7 ± 2.6
−OH	11.7 ± 8.9	90 ± 20	696	9.6 ± 2.4
−C═C	10.0 ± 6.0	180 ± 40	943	11.4 ± 2.8
−COOH	9.3 ± 5.8	180 ± 40	289	12.2 ± 2.6
$-NH_2$	11.7 ± 5.6	340 ± 60	1029	23.4 ± 4.1

[a] Mean force ± std dev computed from 2560 force curves acquired at 10 different locations on the SWNT paper surface. [b] Force per unit radius ± std dev computed from adhesion forces after parsing the data to exclude adhesion measurements from topologically low lying areas. [c] Number of force curves in the parsed data set. [d] Rupture force per molecule ± std dev computed from parsed adhesion force data and the radius of the tip assuming a perfectly ordered, close-packed monolayer.

No clear trend between adhesion force and nature of the thiol end group is apparent.

Close examination of Figure 3 reveals that a direct correlation exists between the topographic and adhesion force images. The highest adhesion forces were observed in areas that are low in the topographical image (in the "valley" between nanotubes) whereas the lowest adhesion forces were observed on the highest regions in the topographical image (along the backbone of a nanotube or bundle). This phenomenon has precedent in adhesion[31,32] and force modulation measurements[33] and is illustrated graphically in Figure 5. Comparison of topographic and force-volume images for all thiol-modified probes investigated herein gave equivalent results; the highest adhesion forces occurred at topologically low areas of the paper. This observation explains why the distribution of forces presented in the histograms of Figure 4 and the first two columns of Table 1 are so broad.

(33) Bar, G.; Rubin, S.; Parikh, A. N.; Swanson, B. I.; Zawodzinski, T. A., Jr.; Whangbo, M. H. *Langmuir* **1997**, *13*, 373−377.

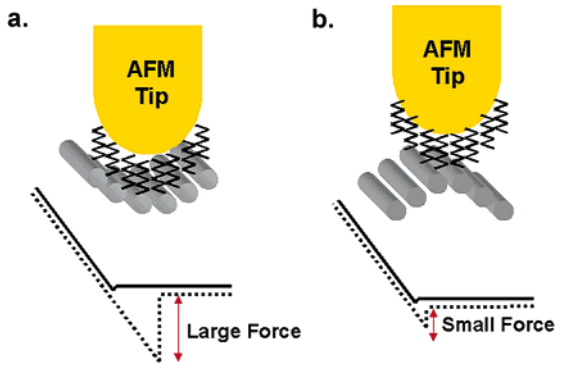

Figure 5. Illustration of the impact of sample topology on the force of adhesion. (a) High adhesion forces are observed when the tip is in contact with a topographically recessed area (i.e., between nanotubes). (b) Low adhesion forces are observed when the tip is in contact with a topographically high area (i.e., along the backbone of a nanotube). Below each illustration is an idealized force curve.

Forces Corrected for Contact Area. To eliminate the contribution of sample topology, the force data were parsed so that data taken from regions of "low" topography were discarded and data taken from regions of "high" topography were retained. The remaining adhesion forces were then compiled for further analysis. Parsing of the data in this manner accounts for the role of the SWNT paper's topology in determining the probe tip−paper contact area; it does not take into account the shape of the tip.

Tip radii of each of the cantilevers used in this study were determined after each adhesion mapping experiment. The cantilever was exposed to oxygen plasma to remove the thiol from the cantilever tip. Then high-resolution (500 nm × 500 nm) Tapping Mode images were acquired at eight locations on the nanotube paper. These images were then processed using commercially available tip-deconvolution software (SPIP by Image Metrology) to provide a measure of the tip radius.

A common approach for comparing adhesion force measurements is to divide the mean adhesive force by the radius of the cantilever tip (F/r).[19,34] The force-to-radius ratio was determined for each thiol-coated tip by dividing the mean adhesion forces from the parsed data set by the radius of the tip. The values obtained as well as the number of force curves in the parsed data set is presented in Table 1. The force-to-radius ratio ranged from a low of 90 pN/nm for the hydroxyl terminus to a high of 340 pN/nm for the amino terminus. While this approach accounts for variations in tip geometry in measured adhesion forces, it does not take into account the number of molecules making contact with the nanotube or their compressibility.

To account for compressibility of the nanotubes and/or the thiol monolayer, we have modeled the contact between the chemically modified probe and the nanotube paper geometrically as a sphere pressing on a cylindrical object. This model suggests that the contact area is elliptical since the radius of contact along the longitudinal axis of the nanotube is larger than the radius of contact along its radial axis. Two expressions can be written from this model, depending upon whether the nanotube compresses under the applied load. If contact of the tip with the nanotube results in compression of the nanotube and the thiol monolayer, then the following equation approximates the surface area contact:

$$\text{contact area} = \frac{\pi^2 r_{NT}(r_{tip}+t)}{2}\,\text{Tan}^1\left(\frac{\sqrt{(r_{tip}+t)^2 - r_{tip}^{\,2} + 4r_{tip}r_{NT} - 4r_{NT}^{\,2}}}{r_{tip}-2r_{NT}}\right) \quad (1)$$

where r_{tip} = radius of the cantilever tip, r_{NT} = the radius of the nanotube, and t = height of thiol. If the nanotube remains uncompressed during contact by the tip but the thiol monolayer is compressed, the following equation describes the area of contact.

$$\text{contact area} \approx \pi^2 r_{NT}\sqrt{2r_{tip}t + t^2} \quad (2)$$

In our experiments, relative triggering was used to limit the maximum pressure applied by the tip on the paper. Given the small size of the probe tip, it was not possible to fully characterize the quality of the alkanethiol monolayer self-assembled onto it. We assumed a densely packed, highly ordered monolayer. The maximum pressure exerted by the tip onto the sample was computed by multiplying the upward deflection of the cantilever at the point of maximum scanner extension multiplied by the spring constant and dividing by the contact area. The applied pressure computed from both equations exceeded the known value for monolayer compression.[35−38] Thus, we conclude that the thiol layer is fully compressed during contact.

Does the nanotube also undergo compression? The calculated pressure exerted on the substrate using the area from eq 2 was 66 MPa. (Note that the contact area for eq 2 is smaller than that from eq 1.) In comparison, the reported pressure to radially compress a single-walled carbon nanotube is ∼1 GPa.[39−41] Thus, we conclude that the pressure used in these experiments was much too small to buckle or compress the nanotubes but large enough to compress the thiol.

Next, to correlate the adhesion force with the terminal group on the thiol, we used the contact area from eq 2 to compute the number of thiols interacting with the nanotube. For this calculation, we assumed a nanotube radius of 0.75 nm was in contact with a densely packed, highly ordered monolayer with a packing density of 4.65 molecules per square nanometer[24,42,43] and a tilt angle of 30° relative to the

(34) Seog, J.; Dean, D.; Plaas, A. H. K.; Wong-Palms, S.; Grodzinsky, A. J.; Ortiz, C. *Macromolecules* **2002**, *35*, 5601−5615.
(35) Salmeron, M.; Folch, A.; Neubauer, G.; Tomitori, M.; Ogletree, D. F. *Langmuir* **1992**, *8*, 2832−2842.
(36) Salmeron, M.; Neubauer, G.; Folch, A.; Tomitori, M.; Ogletree, D. F.; Sautet, P. *Langmuir* **1993**, *9*, 3600−3611.
(37) Thomas, R. C.; Houston, J. E.; Michalske, T. A.; Crooks, C. R. *Science* **1993**, *259*, 1883−1885.
(38) Joyce, S. A.; Thomson, R. C.; Houston, J. E.; Michalske, T. A.; Crooks, C. R. *Phys. Rev. Lett.* **1992**, *68*, 2790−2793.
(39) Salvetat, J.-P.; Briggs, G. A. D.; Bonard, J.-M.; Bacsa, R. R.; Kulik, A. J.; Stockli, T.; Burnham, N. A.; Forro, L. *Phys. Rev. Lett.* **1999**, *82*, 944−947.
(40) Srivastava, D.; Menon, M.; Cho, K. *Phys. Rev. Lett.* **1999**, *83*, 2973−2976.
(41) Wang, Z. L.; Gao, R. P.; Poncharal, P.; de Heer, W. A.; Da, Z. R.; Pan, Z. W. *Mater. Sci. Eng. C* **2001**, *16*, 3−10.

Table 2. Summary of Adhesion Forces between SWNT Paper and the Cantilever Tip Modified with *para*-Substituted Benzenethiols

arylthiol substituent	average rupture force[a] (nN)	force/radius[b] (pN/ nm)	no. of force curves[c]	adhesion force[d] (pN/molecule)
$-CH_3$	3.5 ± 2.0	220 ± 60	873	18.9 ± 5.6
$-NO_2$	2.7 ± 2.1	260 ± 60	1735	21.8 ± 5.3
$-NH_2$	3.5 ± 2.3	410 ± 80	1580	22.6 ± 4.7
$-Br$	4.2 ± 2.5	230 ± 30	649	26.9 ± 3.6
$-OH$	5.5 ± 2.7	550 ± 140	1044	32.0 ± 8.4
$-F$	3.9 ± 2.3	390 ± 090	1436	39.5 ± 8.8
$-OCH_3$	4.1 ± 2.1	580 ± 150	1531	41.5 ± 10.9
$-H$	4.4 ± 2.8	520 ± 130	1256	46.8 ± 11.8
$-C\equiv N$	5.7 ± 2.5	660 ± 180	1392	56.9 ± 15.4

[a] Mean force ± std dev computed from 2560 force curves acquired at 10 different locations on the SWNT paper surface. [b] Force per unit radius ± std dev computed from adhesion forces after parsing the data to exclude adhesion measurements from topologically low lying areas. [c] Number of force curves in the parsed data set. [d] Rupture force per molecule ± std dev computed from parsed adhesion force data and the radius of the tip assuming a perfectly ordered, close-packed monolayer.

surface normal.[44,45] The adhesion force per molecule was computed for each thiol from the parsed data set and is also listed in Table 1. Adhesion forces ranged from 7.6 pN per molecule for the methyl-terminated alkanethiol to 23.4 pN per molecule for the amino-terminated alkanethiol. The latter finding correlates with previous reports of SWNTs having a higher propensity to "stick" on a surface modified with amine-terminated molecules.[46] The affinity of the alkanethiol decreases in the following order: $-NH_2 > -COOH > -C{=}C > -OH > -CF_3 \approx -SH > -CH_3$.

Adhesion of Arylthiols to SWNT Paper. Force volume experiments were also conducted using tips chemically modified with a series of *para*-substituted benzenethiols. Adhesion maps and histograms of adhesion forces for each of these are presented in the Supporting Information. Pertinent results from this set of experiments are listed in Table 2. The average rupture force ranged from 2.7 ± 2.1 nN for *para*-nitrobenzenethiol to 5.7 ± 2.5 nN for *para*-cyanobenzenethiol and is smaller than that observed for the alkanethiol series. The data were parsed to remove topologically induced dispersion and the shape of the probe tips was determined in the same manner as described above for the alkanethiol series. Force-to-radius ratios were computed from the parsed data and ranged from 220 pN/nm for the *para*-methylbenzenethiol to 660 pN/nm for the *para*-cyanobenzenethiol. To compute the adhesion force per molecule, we again assumed a nanotube radius of 0.75 nm in contact with a densely packed, highly ordered monolayer 0.7 nm in height with a packing density of 3.07 molecules/nm^2.[47−50] The

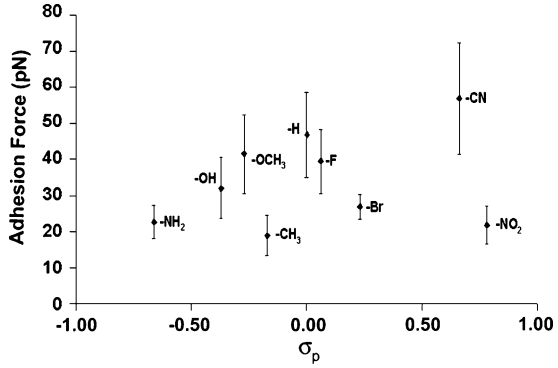

Figure 6. Plot of the adhesion force per molecule versus the corresponding Hammett parameter of a *para*-substituted benzenethiol molecule.

computed adhesion force per arylthiol molecule is given in Table 2. Adhesion forces ranged from 18.9 pN/molecule for methylbenzenethiol to 56.9 pN/molecule for the cyanobenzenethiol. The trend in the adhesion force per molecule for the *para*-substituted benzenethiols is: $-C\equiv N > -H > -OCH_3 > -F > -OH > -Br > -NH_2 > -NO_2 > -CH_3$. The adhesion forces for the arylthiols are significantly higher than those observed for the alkanethiols. This finding suggests significant interaction between the nanotube and the benzene ring at the point of compression and supports our claim of a compressible monolayer.

As a predictive tool, we have attempted to correlate the observed adhesion force per molecule with a variety of parameters including the hardness (η), ionization potential[51] (I), and Hammett constant[52] (σ_p^+) for the benzenethiol substituents. The plot of the adhesion force per molecule versus the Hammett constant is depicted in Figure 6. (Note: correlation of hardness and ionization potential with adhesion force is provided in the Supporting Information.) A somewhat linear relationship is found. Electron-withdrawing substituents on the arylthiol display higher adhesive interactions with the sidewalls of the nanotube compared to electron-donating substituents. It is interesting to note that Star and co-workers have recently found a linear relationship between the gate voltage modulation of a SWNT-based field-effect transistor and the Hammett substituent constant for *para*-substituted benzenes with many of the same substituents as used herein for the *para*-substituted benzenethiols.[53] We suggest that the lack of a linear relationship in Figure 6 may be due to defects in the monolayer, improper assessment of the area per molecule, or differences in the packing density from one arylthiol to another. Similarly, correlation of the adhesion force for the alkanethiols with the electronegativity of the terminal group was attempted. No well-defined trend was observed.

Our findings demonstrate that the interfacial interactions between SWNT paper and terminally substituted hydrocarbons can be evaluated with an AFM, provided that one accounts for variations in contact area caused by tip shape and sample topology. In a broader context, our findings

(42) Chidsey, C. E. D.; Loiacono, D. N. *Langmuir* **1990**, *6*, 682−691.
(43) Ulman, A. *Chem. Rev.* **1996**, *96*, 1533−1554.
(44) Nuzzo, R. G.; Dubois, L. H.; Allara, D. L. *J. Am. Chem. Soc.* **1990**, *112*, 558−569.
(45) Dubois, L. H.; Nuzzo, R. G. *Annu. Rev. Phys. Chem.* **1992**, *43*, 437−463.
(46) Liu, J.; Casavant, M. J.; Cox, M.; Walters, D. A.; Boul, P.; Lu, W.; Rimberg, A. J.; Smith, K. A.; Colbert, D. T.; Smalley, R. E. *Chem. Phys. Lett.* **1999**, *303*, 125−129.
(47) Ruths, M. *Langmuir* **2003**, *19*, 6788−6795.
(48) Nielsen, J. U.; Esplandiu, M. J.; Kolb, D. M. *Langmuir* **2001**, *17*, 3454−3459.
(49) Tao, Y.-T.; Wu, C.-C.; Eu, J.-Y.; Lin, W.-L.; Wu, K.-C.; Chen, C.-h. *Langmuir* **1997**, *13*, 4018−4023.
(50) Jin, Q.; Rodriguez, J. A.; Li, C. Z.; Darici, Y.; Tao, N. J. *Surf. Sci.* **1999**, *425*, 101−111.
(51) Parr, R. G.; Pearson, R. G. *J. Am. Chem. Soc.* **1983**, *105*, 7512−7516.
(52) Hansch, C.; Leo, A.; Taft, R. W. *Chem. Rev.* **1991**, *91*, 165−195.
(53) Star, A.; Han, T.-R.; Gabriel, J.-C. P.; Bradley, K.; Gruener, G. *Nano Lett.* **2003**, *3*, 1421−1423.

suggest that surface adhesive force measurements based on multiple force curves taken at a single point on the surface or based on the interpretation of single-force curves acquired at different locations on the surface may be subject to a systematic error resulting from variations in contact area. Second, surface adhesive force measurements acquired using multiple force curves acquired at several points on the surface without consideration of the compliance of the surfaces may also be subject to errors resulting from variations in contact area. Contact area assessment requires characterization of tip shape, consideration of sample topography, and careful examination of the compliance of both surfaces.

We are continuing in our effort to assess interfacial interactions with the sidewalls of carbon nanotubes. Force−volume imaging experiments under liquid are currently underway to ascertain the role of hydration layers on the tip and substrate in interfacial adhesion. In another experiment, we are bringing a nanotube attached to a tip in contact with a chemically modified substrate.[54] In this experiment, uncertainty in the contact area will be dramatically reduced since the measured adhesive force should be proportional to the length of tube in contact with the underlying surface. Also, there will be no compression of the nanotube upon contact with the modified substrate. The results of these experiments and the insights gained from them will be reported in due course.

In conclusion, chemical force microscopy has been used to probe the local adhesion between substituted alkane- and arylthiol molecules and the sidewalls of single-walled nanotubes. The results reported herein suggest that polymers comprised of aryl groups with electron-withdrawing substituents should exhibit stronger interfacial interactions with the sidewalls of carbon nanotubes compared to polymers comprised of extended alkyl moieties. Greater interfacial interaction should result in reduced nanotube aggregation and increased mechanical strength. It is anticipated that the information presented herein will be of direct utility in designing polymer/nanotube composite materials with improved properties.

Acknowledgment. M.A.P. would like to acknowledge support from the NASA Graduate Student Researchers Program (NGT-1-02002). Partial support of this research from NIH (Grant EB000767) is gratefully acknowledged.

Supporting Information Available: Additional figures showing highly pixelated topographical images, histograms, and plot of adhesion force per molecule (PDF). This material is available free of charge via the Internet at http://pubs.acs.org.

CM048346M

(54) Poggi, M. A.; McFarland, A. E.; Lillehei, P. T.; Colton, J. S.; Bottomley, L. A. *Nanotechnology*, **2005**, submitted for publication.